The Journal of Physical Chemistry A

 VOLUME 103, NUMBER 12, MARCH 25, 1999

LETTERS

UV Photolysis of ClOOCl

Teresa A. Moore and Mitchio Okumura*

Arthur Amos Noyes Laboratory of Chemical Physics, Mail Stop 127-72, California Institute of Technology, Pasadena, California 91125

James W. Seale and Timothy K. Minton*

Department of Chemistry and Biochemistry, Montana State University, Bozeman, Montana 59717

Received: November 11, 1998; In Final Form: February 2, 1999

ClOOCl (ClO dimer) photolysis is believed to dominate the catalytic destruction of polar stratospheric ozone during springtime through the production of atomic chlorine. Decomposition by an alternate pathway to form ClO would not catalyze ozone loss. Molecular beam experiments have demonstrated that photoexcitation of ClOOCl at both 248 and 308 nm leads to dissociation via multiple dynamical pathways, producing ClO + ClO and 2Cl + O_2. At 248 nm, both concerted and sequential dissociation to 2Cl + O_2 were observed. The primary dissociation channels occurred within a rotational period at both excitation wavelengths. The relative Cl:ClO product yields are 0.88:0.12 and 0.90:0.10 at 248 and 308 nm, respectively. Lower limits on these ratios were determined. These results substantially confirm the importance of ClOOCl photolysis in catalyzing springtime polar ozone depletion.

The large springtime depletion of stratospheric ozone over the Poles is thought to be catalyzed primarily by the photolysis of ClOOCl. Chlorine atoms released through ClOOCl dissociation participate in ozone loss through the photochemical cycle:[1]

$$\mathrm{ClO + ClO + M \rightarrow ClOOCl + M} \quad (1)$$

$$\mathrm{ClOOCl} + h\nu \rightarrow \mathrm{ClOO + Cl} \quad (2)$$

$$\mathrm{ClOO + M \rightarrow Cl + O_2 + M} \quad (3)$$

$$2[\mathrm{Cl + O_3 \rightarrow ClO + O_2}] \quad (4)$$

$$\text{net: } 2\mathrm{O_3 \rightarrow 3O_2}$$

In current models, this catalytic cycle accounts for 70−80% of the ozone loss over Antarctica. However, if photolysis of ClOOCl results in cleavage of the weakest (peroxy) bond to form ClO products, then the consequent null cycle would not deplete ozone. The branching ratio between Cl and ClO products from ClOOCl photolysis is therefore critical in determining the effectiveness of this mechanism for destroying ozone.

ClOOCl has a strong, broad absorption centered at 245 nm. Absorption in the 305−400 nm tail leads to photolysis in the stratosphere during the polar spring.[2] When ClOOCl is excited in the UV (E_{phot} = 265−500 kJ/mol), it can dissociate via several channels, including[3]

$$\mathrm{ClOOCl} + h\nu \rightarrow \mathrm{ClO + ClO} \quad \Delta H_0^\circ = 71.5 \text{ kJ/mol} \quad (5)$$

$$\rightarrow \mathrm{ClOO + Cl} \quad = 88.7 \text{ kJ/mol} \quad (6)$$

$$\rightarrow \mathrm{2Cl + O_2} \quad = 108.4 \text{ kJ/mol} \quad (7)$$

$$\rightarrow \mathrm{Cl + O + ClO} \quad = 336.8 \text{ kJ/mol} \quad (8)$$

The NASA Data Evaluation Panel[4] currently recommends a unit quantum yield for reaction 6, based on high quantum yields for

* To whom correspondence should be addressed.

10.1021/jp984410+ CCC: $18.00
Published on Web 03/04/1999

total Cl-atom production (Φ_{Cl}) observed in two experiments. Cox and Hayman[5] examined this process indirectly by steady-state photolysis of Cl_2O at 254 nm in a static cell. They inferred the presence of ClOOCl from a kinetics model and deduced $\Phi_{Cl} = 3.8 \pm 1.6$ for ClOOCl photolysis. Molina et al.[6] used resonance fluorescence to measure the Cl-atom yield directly from ClOOCl photolysis at 308 nm in a flow tube and found $\Phi_{Cl} = 2.06 \pm 0.24$. They detected no ClO products with an NO titration method, consistent with the observed Cl yield. However, the calculation of Φ_{Cl} depended upon the ratio of the ClOOCl absorption cross sections at 245 and 308 nm, for which literature values[3,7] vary from 13 to 22. If recalculated, Φ_{Cl} could range from 1.2 to 2.06. Both groups reported no evidence for the ClOO intermediate, and neither could distinguish between final product channels 2 and 7. These uncertainties are significant enough to alter quantitatively model predictions of polar stratospheric ozone loss.

The 245 nm absorption band arises from transitions to antibonding σ^* (ClO) orbitals,[2] which led to suggestions that ClOOCl photolysis would result only in Cl−O bond fission. However, a bond-selective model of photodissociation can be too simplistic. In a study of $ClONO_2$ photolysis, we showed[8] that cleavage of the weaker $ClO-NO_2$ bond competes effectively with Cl−O bond fission following excitation to a σ^* orbital localized on the ClO chromophore. On the basis of these results, we raised the possibility that there might be a significant yield of ClO products in ClOOCl photolysis.

We report here a molecular beam experiment on the photolysis of ClOOCl at two wavelengths, 248 and 308 nm, which employed photofragment translational spectroscopy as in our $ClONO_2$ studies. We have directly observed Cl, ClO, and O_2 photofragments by mass spectrometric detection. The relative yields of Cl and ClO products have been determined by calibrating the relative detector sensitivity for ClO and Cl with a Cl_2O photolysis experiment.[9]

The experiments were performed on a crossed molecular beams apparatus[10] modified for laser photolysis. A molecular beam of ClOOCl was crossed at right angles with the UV radiation from a pulsed excimer laser focused at the interaction region. The photolysis products were detected off the beam axis by a mass spectrometer that is rotatable in the plane of the laser and molecular beams. Product time-of-flight (TOF) distributions were collected at various detector angles for each photofragment mass-to-charge ratio (m/z) as a function of time. A forward convolution technique[8] was used to determine the center-of-mass (c.m.) translational energy and angular distributions for each two-body dissociation channel. The angular distribution is characterized by the anisotropy parameter β,[11] which can range from $\beta = -1$ for a transition with the dipole perpendicular to the recoil vector to $\beta = 2$ for a pure parallel transition.

Production of a beam of ClOOCl was key to the feasibility of this experiment, which required partial pressures of ClOOCl ($p_{ClOOCl} \approx 1-2$ Torr) 1−2 orders of magnitude higher than had been reported in the literature. We formed ClOOCl by recombination of ClO (eq 1). This method is known to produce primarily ClOOCl rather than other Cl_2O_2 isomers.[12] After extensive photochemical modeling, we chose to generate high transient concentrations of ClO radicals ($p_{ClO} > 3$ Torr) by 308-nm photolysis of Cl_2O in the high-pressure stagnation region. Cl_2O (10 Torr) was seeded in a buffer of 2% SF_6 in He at a total pressure of 190 Torr. The initial temperature was kept below 220 K to prevent the ClO self-reaction. Modeling indicated that most of the ClO reacted during the 300−500 μs residence time prior to expansion through a 100 μm nozzle. The beam velocity was typically 9.5×10^4 cm/s. Mass spectrometric analysis[13] confirmed that approximately 1.5 Torr of ClOOCl was formed. However, Cl_2, Cl_2O, and ClO were also present with average abundances of 6, 0.4, and 0.06 relative to ClOOCl. Although there was a strong signal at $OClO^+$, crossed-beam nonreactive scattering measurements with Ne confirmed that this signal arose from ionizer fragmentation of Cl_2O_2 or heavier species. A weak $Cl_2O_3^+$ signal (<6% of $Cl_2O_2^+$) indicated the presence of either small quantities of Cl_2O_3 or low relative concentrations of clusters. These results corroborated model predictions of insignificant OClO and Cl_2O_3 concentrations.

Light at 248 and 308 nm can photolyze the three major impurities (Cl_2, Cl_2O, and ClO) to form Cl and ClO photofragments. We performed separate photolysis experiments on Cl_2 and Cl_2O at both wavelengths to obtain their translational energy and angular distributions, which allowed us to model their contributions to the observed photolysis signal. Photolysis of any clusters would likely result in Cl or ClO photofragments with low c.m. translational energies (E_T).

Examples of TOF spectra are shown in Figure 1 for 248 nm and Figure 2 for 308 nm excitation. The signal-to-noise ratio at 308 nm was less than that at 248 nm because the relative ClOOCl absorption cross section is ~18 times lower.[7] Regardless of excitation wavelength, the largest signal was observed at $m/z = 35$ (Cl^+) and a significant signal was still seen at $m/z = 51$ (ClO^+). No products were detected at $m/z = 67$ (ClO_2^+). We also observed a fast O_2^+ signal at 248 nm.

The ClO^+ TOF distributions (Figure 1A) obtained in the experiment at 248 nm consisted of overlapping signals from ClO products of Cl_2O and ClOOCl photodissociation. Although the data looked similar to the ClO^+ signal predicted for Cl_2O alone, the Cl_2O photoproduct signal was somewhat faster than that in the observed TOF spectrum, as shown in Figure 3. By matching the predicted Cl_2O product signal to the rising edge of the observed signal, we found that Cl_2O photolysis accounted for ~50% of the ClO^+ signal. The remaining ClO^+ signal gave a bimodal peak (dashed line, Figure 1A) which we assigned to ClO products from $ClOOCl + h\nu \rightarrow ClO + ClO$ with an average total internal energy $\langle E_{int} \rangle$ of 310 kJ/mol and anisotropy parameter $\beta = 0.5$. A slower ClO^+ peak was also observed, which we assigned to a minor channel:[14] $ClO(X) + ClO(A) \rightarrow ClO(X) + Cl + O(^3P)$.[15] There were several contributions to the Cl^+ TOF distributions (Figure 1B) at 248 nm, but only a small fraction of the signal could be attributed to photolysis of impurities. Photolysis of ClO[16] gave rise to a single peak (thin solid line, Figure 1B). We determined the Cl^+ contribution from photolysis of Cl_2O (short-dashed line, Figure 1B) from the known Cl^+:ClO^+ relative intensities for pure Cl_2O photolysis. We also accounted for the signal at this m/z from the ClO products from reaction 5, which underwent fragmentation to Cl^+ in the ionizer.[17] We modeled the remaining Cl^+ signal as Cl-atom products from ClOOCl photolysis. The main peak (160 μs, dot-dot−dashed line, Figure 1B) matched the expected TOF distribution for Cl atoms recoiling with a total momentum equal and opposite to that of the O_2^+ fragments (105 μs, Figure 1C) if we assumed that both Cl−O bonds broke nearly simultaneously. We therefore assigned this peak and the corresponding O_2^+ signal to the concerted dissociation to $2Cl + O_2$. The best fits were obtained with an assumed dissociation geometry similar to the ground-state geometry but with a smaller dihedral angle (65° instead of 81°). The high translational energy release, on average 72% of the available energy, is characteristic of a concerted process.[18] The angular distributions gave anisotropy parameters $\beta_{O_2} = -1.0$ and $\beta_{Cl} = 0.1$. For a primary two-body

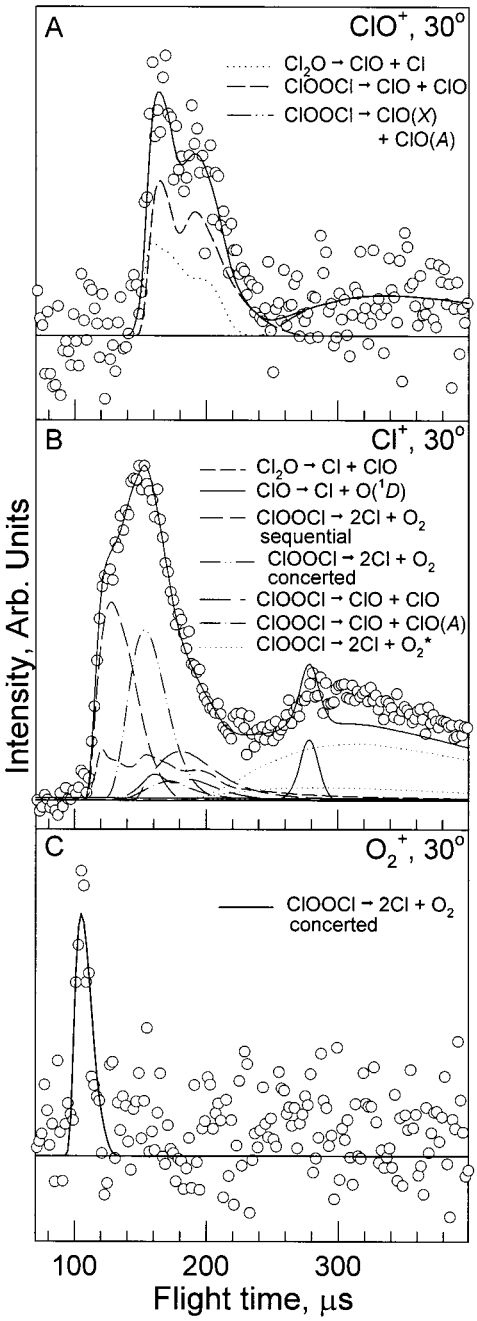

Figure 1. Time-of-flight (TOF) distributions for products from ClOOCl photolysis at 248 nm. TOF spectra were collected at a detector angle of 30° for (A) ClO^+, (B) Cl^+, and (C) O_2^+ fragments. The contribution in B from the ClO + ClO product channel arises from fragmentation to Cl^+ in the ionizer, and the contribution from the ClO + ClO(*A*) channel arises from predissociation of the ClO(*A*).

dissociation, the β parameters should be identical. The fact that they are different and of opposite sign is strong evidence that the dissociation is concerted.[19] After subtracting this main peak, both a faster and slower signal remained. We assigned the faster peak to primary Cl atoms from the Cl + ClOO channel (long-dashed line, 125 μs, Figure 1B). The angular distribution gave an anisotropy parameter of $\beta = 0.6$. No $ClOO^+$ signal was observed, indicating that all ClOO products dissociated. This result is not surprising, because the internal energy of the ClOO fragment ($\langle E_{int} \rangle = 276$ kJ/mol) was far in excess of its dissociation energy ($D_0 \approx 20$ kJ/mol). We modeled the secondary dissociation[20] of ClOO assuming formation of ground-state Cl + O_2 products to obtain the contribution to the slow shoulder of the main Cl^+ peak (long-dashed line, 185 μs, Figure 1B). The observed spectra could not be fit using RRKM theory. Finally, the slowest peak in the Cl^+ distribution (dotted lines, Figure 1A) was modeled as a unimolecular decay[21] via a Cl + ClOO* channel to Cl and electronically excited O_2 ($^1\Delta$) products.

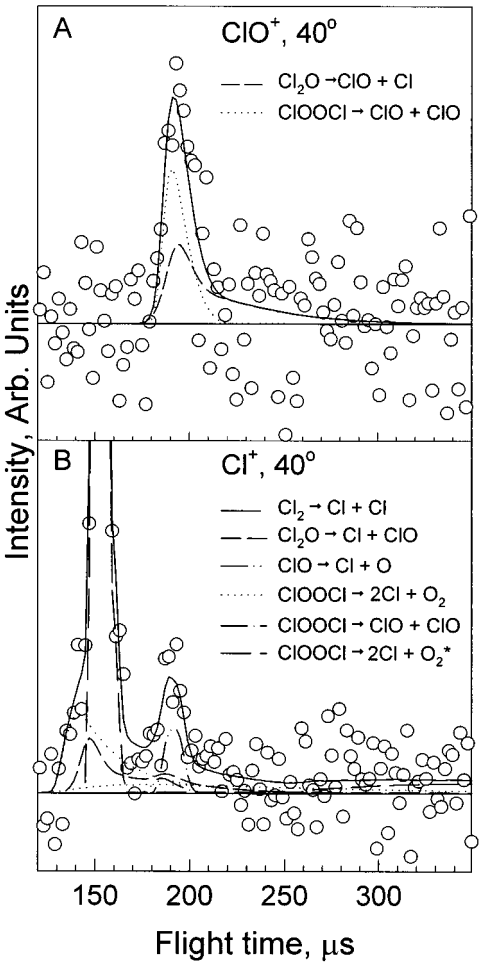

Figure 2. TOF distributions for products from ClOOCl photolysis at 308 nm. TOF spectra were collected at a detector angle of 40° for (A) ClO^+ and (B) Cl^+ fragments. The contribution in B from the ClO product channel arises from fragmentation to Cl^+ in the ionizer.

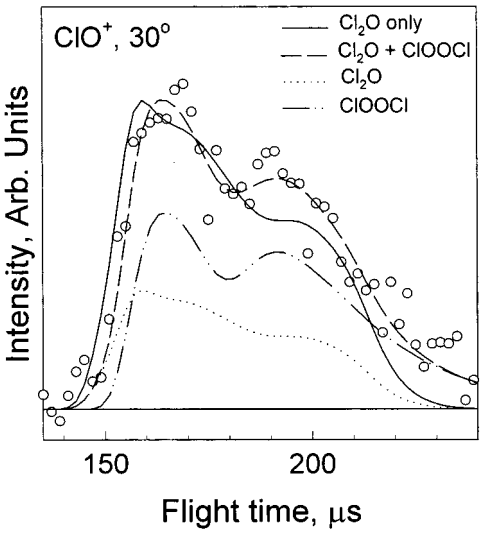

Figure 3. ClO^+ TOF distribution of products photolyzed at 248 nm and collected at a detector angle of 30°. The solid line denotes the fit if the ClO^+ products arise solely from Cl_2O photolysis.

TABLE 1: Relative Yields for the ClOOCl Photolysis Channels Observed at 248 and 308 nm

	248 nm		308 nm	
	relative yield	β	relative yield	β
Dynamical Channels				
i. $Cl + ClOO \rightarrow Cl + Cl + O_2$	0.55	0.6	0.5	1.5
ii. $Cl + O_2 + Cl$ (concerted)	0.18	$\beta_{O_2} = -1.0$ $\beta_{Cl} = 0.1$		
iii. $ClO + ClO$	0.09	0.5	0.1	2.0
iv. $Cl + ClOO^* \rightarrow Cl + Cl + O_2^*$	0.14	0.0	0.4	0.0
v. $ClO + ClO^* \rightarrow ClO + Cl + O$	0.04	0.0		
Relative Product Yields[a]				
$2Cl + O_2$	0.88 ± 0.07 (0.89)		0.90 ± 0.1 (0.83)	
$ClO + ClO$	0.12 ± 0.07 (0.11)		0.10 ± 0.1 (0.17)	
branching ratio† Cl:ClO:O	1.0:0.15:0.02 (1.0:0.13:0.00)		1.0:0.11:0.0 (1.0:0.20:0.0)	

[a] Yields and ratios in parentheses are calculated assuming that products with low center-of-mass translational energies (c.m. E_T) are assigned to cluster photodissociation rather than channels iv and v.

We observed contributions to the photolysis signal at 308 nm from ClO, Cl_2, Cl_2O, and ClOOCl as shown in Figure 2. We could not unambiguously determine the contributions from ClO[22] or Cl_2O photolysis based on the TOF data at either m/z. The Cl^+ TOF spectrum was dominated by dissociation of Cl_2 (long-dashed line, Figure 2B). We therefore estimated the Cl_2O (short-dashed line) and ClO (dot−dot−dashed lines) contributions relative to the Cl_2 peak (long-dashed line) based on abundances determined by mass spectrometer measurements.[23] The Cl_2O contribution to the ClO^+ signal was then obtained from known Cl^+:ClO^+ relative intensities. This analysis was consistent for different source conditions under which the relative abundances varied by as much as a factor of 4.

Significant ClO^+ signal remained (∼30−60%), which we assigned to $ClOOCl + h\nu \rightarrow ClO + ClO$ (dotted line, Figure 2A). The ClO products were vibrationally excited ($\langle$total $E_{int}\rangle$ = 201 kJ/mol). The angular distribution indicated a parallel transition ($\beta = 2.0$).

Cl^+ signal also remained after accounting for contributions from photolysis of impurities and fragmentation in the ionizer of ClO products. We assigned the fast shoulder at 135 μs (dotted line, Figure 2B) to primary Cl from the $ClOOCl \rightarrow Cl + ClOO$ channel and the slower broader signal to Cl atoms from the secondary process $ClOO \rightarrow Cl + O_2$ (dotted line, Figure 2B). We again interpreted the absence of ClO_2^+ product signal as an indication that the ClOO counterfragment, formed with $\langle E_{int}\rangle$ = 184 kJ/mol, spontaneously dissociated. The angular distribution for the primary Cl gave $\beta = 1.5$. High background at m/z = 32 (O_2^+) prevented us from identifying a concerted $2Cl + O_2$ channel. A slow signal was observed at $m/z = 35$ but not at $m/z = 51$. This slow Cl^+ signal, centered at 330 μs, was much larger in proportion to the fast $Cl + ClOO$ signal than it was at 248 nm. We again modeled this signal as a statistical (RRKM) dissociation to $Cl + ClOO^* \rightarrow Cl + O_2^*$.

Table 1 gives the relative yields of the primary dissociation channels for both wavelengths.[24] Although we observe products from multiple dissociation pathways, ultimately there are two main product channels: $2Cl + O_2$ and $ClO + ClO$. Their relative yields may be interpreted as absolute quantum yields, because excitation into strong, broad UV absorption bands typically results in dissociation with unit quantum efficiency. As seen by the Cl:ClO product ratios (Table 1), chlorine atoms are the dominant products (> 85%) upon photolysis at both wavelengths. A small O-atom yield at 248 nm is inferred from ClO(A) predissociation from the possible ClO(X) + ClO(A) channel.

Although we assign the products with low c.m. E_T to ClOOCl photolysis channels, we cannot exclude the possibility that these products are formed by cluster dissociation; however, these are minor products whose assignments have little effect on the Cl:ClO yields. If we attribute the low c.m. E_T products to clusters rather than channels iv and v (Table 1), the resulting product yields and branching ratios (given in parentheses in Table 1) are unaffected within the experimental uncertainty.

The observation of multiple dissociation pathways, including peroxy-bond fission, suggests that a simple bond-selective picture is inadequate. More striking is the occurrence at 248 nm of both concerted and sequential cleavage of the two Cl−O bonds. Furthermore, we conclude from the anisotropies of the two $2Cl + O_2$ channels that different electronic states are initially excited. Several excited states have been predicted, but more detailed calculations of the excited-state surfaces are needed to explain the observed dynamics.

The ClO yield in Table 1 is based on our best estimate of the signal from Cl_2O photolysis, but we can place a strict upper limit on the ClO yield if we assume that all of the ClO^+ signal is from $ClOOCl \rightarrow ClO + ClO$. In this case, the relative ClO:Cl branching ratio can be no greater than 0.19:0.81 at 248 nm and 0.31:0.69 at 308 nm.[25] Hence, $ClO + ClO$ is at most a minor product channel from ClOOCl photolysis at 248 and 308 nm. Alternatively, we can assign all of the ClO^+ signal to Cl_2O photolysis, but the poor fits indicate that this assignment is unlikely.

Photolysis of other isomers of Cl_2O_2 could conceivably contribute to the observed signal; however, ClOOCl is the most stable isomer, with chloryl chloride ($ClClO_2$) and chlorine chlorite (ClOClO) less stable by 4 and 40 kJ/mol, respectively.[26] Furthermore, we produce ClOOCl at high pressures by the three-body recombination reaction 1, which is known[12] to generate predominately the ClOOCl isomer.[27] Although we cannot entirely rule out the presence of other isomers, the source chemistry favors ClOOCl as the dominant isomer present in our experiment.

Our results support the previous reports[5,6] that the stronger Cl−O bond is preferentially broken and that Cl atoms are the dominant products from UV photolysis of ClOOCl. The absolute quantum yield determined by Molina et al. at 308 nm depends on the ClOOCl absorption cross section. The most recent absorption cross-section measurement[7] results in a recalculated yield for the $2Cl + O_2$ channel (7) at 308 nm of $\Phi_7 = 0.88$, in good agreement with our results ($\Phi_7 = 0.9$). Furthermore, the high ClO vibrational excitation that we observe could explain their inability to detect ClO products. Recent experiments show that their detection method, titration with NO, is less efficient than assumed when ClO is vibrationally excited.[28]

We conclude from our results at 308 nm that in the stratosphere

$$\mathrm{ClOOCl} + h\nu \rightarrow 2\mathrm{Cl} + \mathrm{O_2} \qquad \Phi_7 = 0.9 \pm 0.1 \qquad (7)$$

$$\rightarrow \mathrm{ClO} + \mathrm{ClO} \qquad \Phi_5 = 0.1 \pm 0.1 \qquad (5)$$

with an absolute upper limit of $\Phi_5 = 0.31$ for the ClO product channel. The intermediate ClOO (reaction 6) is formed with $E_{\mathrm{int}} \gg D_0$ and likely dissociates spontaneously under stratospheric conditions. The high Cl yield we observed implies that the catalytic cycle involving photolysis of ClOOCl is an important mechanism for ozone loss under perturbed polar conditions. Further modeling studies are necessary to determine whether the small ClO yield observed would require additional ozone loss mechanisms to balance the ozone budget, especially in the Arctic vortex where modeling underestimates ozone loss rates.

Acknowledgment. This work was supported by NASA/UARP Grant Nos. NAGW-3893 and NAG5-3911; calculations were performed with support of the JPL Supercomputing Project. We are grateful to Christine M. Nelson, Donna J. Garton, and Thomas S. Schindler for experimental assistance.

References and Notes

(1) Molina, L. T.; Molina, M. J. *J. Phys. Chem.* **1987**, *91*, 433.

(2) Stanton, J. F.; Bartlett, R. J. *J. Chem. Phys.* **1993**, *98*, 9335.

(3) $\Delta H_f°(0\mathrm{K})_{\mathrm{ClOOCl}} = 31.2$ kcal/mol from Nickolaisen, S. L.; Friedl, R. R.; Sander, S. P. *J. Phys. Chem.* **1994**, *98*, 155.

(4) DeMore, W. B.; Sander, S. P.; Golden, D. M.; Hampson, R. F.; Kurylo, M. J.; Howard, C. J.; Ravishankara, A. R.; Kolb, C. E.; Molina, M. J. *Chemical Kinetics and Photochemical Data for Use in Stratospheric Modeling, Evaluation Number 12*; JPL Publication 97-4, JPL, 1997.

(5) Cox, R. A.; Hayman, G. D. *Nature* **1988**, *332*, 796.

(6) Molina, M. J.; Colussi, A. J.; Molina, L. T.; Schindler, R. N.; Tso, T.-L. *Chem. Phys. Lett.* **1990**, *173*, 310.

(7) Huder, K. J.; DeMore, W. B. *J. Phys. Chem.* **1995**, *99*, 3905.

(8) Minton, T. K.; Nelson, C. M.; Moore, T. A.; Okumura, M. *Science* **1992**, *258*, 1342. Moore, T. A.; Okumura, M.; Tagawa, M.; Minton, T. K. *Faraday Discuss. Chem Soc* **1995**, *100*, 295. Nelson, C. M.; Moore, T. A.; Okumura, M.; Minton, T. K. *Chem. Phys.* **1996**, *207*, 287.

(9) Nelson, C. M.; Moore, T. A.; Okumura, M.; Minton, T. K. *J. Chem. Phys.* **1994**, *100*, 8055. Moore, T. A.; Okumura, M.; Minton, T. K. *J. Chem. Phys.* **1997**, *107*, 3337.

(10) Lee, Y. T.; McDonald, J. D.; LeBreton, P. R.; Herschbach, D. R. *Rev. Sci. Instrum.* **1969**, *40*, 1402.

(11) The anisotropy parameter β is given by $\beta = 2P_2(\cos\chi)$, where P_2 is the second Legendre polynomial and χ is the angle between the electronic transition moment and the center-of-mass recoil axis of the fragments. Busch, G. E.; Wilson, K. R. *J. Chem. Phys*. **1972**, *56*, 3626.

(12) Schwell, M.; Jochims, H.-W.; Wassermann, B.; Rockland, U.; Flesch, R.; Rühl, E. *J. Phys. Chem.* **1996**, *100*, 10700.

(13) The nominal electron energy was lowered to 30 eV in order to reduce fragmentation.

(14) ClO(A) spontaneously predissociates to produce Cl and O(^3P) atoms.

(15) The translational energy distribution was obtained by a fit to an RRKM mechanism with $\beta = 0$.

(16) Davis, H. F.; Lee, Y. T. *J. Phys. Chem.* **1996**, *100*, 30. To fit our ClO photolysis signal (the thin solid line at 240 μs in Figure 1B) at 248 nm, a value of $\beta = 2.0$ was needed.

(17) The fragmentation of ClO from Cl_2O photolysis was determined based on the pure Cl_2O photolysis experiments, which had three ClO components with differing average internal energies. The fragmentation of ClO from ClOOCl photolysis was determined based on the average internal energy of the ClO and knowledge of the Cl_2O fragmentation pattern.

(18) Maul, C.; Gericke, K.-H. *Int. Rev. Phys. Chem.* **1997**, *16*, 1.

(19) Baum, G.; Felder, P.; Huber, R. J. *J. Chem. Phys.* **1993**, *98*, 1999. Wannenmacher, E. A. J.; Felder, P.; Huber, J. R. *J. Chem. Phys.* **1991,** *95*, 986.

(20) At $m/z = 32$, the signal-to-noise ratio was very low due to high O_2 background. The slower, broader signal from the secondary dissociation of ClOO was not detectable.

(21) An RRKM calculation was used to model this dissociation process.

(22) At 308 nm, ClO photodissociated to Cl($^2P_{3/2,1/2}$) + O(^3P) and was observed at 195 μs in Figure 2B.

(23) We estimated the relative abundances of ClO, Cl_2, and Cl_2O from the beam mass spectrometric measurements, their relative electron impact ionization cross sections, and their ionizer fragmentation patterns (observed in Cl_2 and Cl_2O photolysis experiments and estimated for ClO). The expected contributions to the Cl^+ photolysis signal were then determined from the relative absorption cross sections at 308 nm.

(24) The relative yield for the concerted channel was determined from a primary c.m. flux distribution that was obtained by modeling the Cl products as arising from a primary two-body channel.

(25) Some ClO photofragments could go undetected if they absorbed a second photon and dissociated, but the photolysis laser fluence was kept low enough to minimize this process. Under these conditions, little ClO photodissociation was observed in the Cl_2O photolysis experiments.

(26) Lee, T. J.; Rohlfing, C. M.; Rice, J. E. *J. Chem. Phys.* **1992**, *97*, 6593. Stanton, J. F.; Rittby, C. M. L.; Bartlett, R. J.; Toohey, D. W. *J. Phys. Chem.* **1991**, *95*, 2107. McGrath, M. P.; Clemitshaw, K. C.; Rowland, F. S.; Hehre, W. H. *Geophys. Res. Lett.* **1988**, *15*, 883. Jensen, F.; Oddershede, J. *J. Phys. Chem.* **1990**, *94*, 2235.

(27) While the ClOClO isomer could form from ClO clustering in the nozzle expansion, the ClO concentration in the stagnation region was so low (~30 mTorr) that this process can be neglected.

(28) Tyndall, G. S.; Kegley-Owen, C. S.; Orlando, J. J.; Calvert, J. G. *J. Chem. Soc., Faraday Trans.* **1997**, *93*, 2675.